2024 IEEE/RSJ International Conference on Intelligent Robots and Systems (IROS)
October 14-18, 2024. Abu Dhabi, UAE

A Robotic Mediation Device for Skill Assessment and Training During Colonoscopy

Olivia Richards[1], Elan Ahronovich[1], Neel Shihora[1], Ahmet Yildiz[1], Jumana Atoum[2], Jie Ying Wu[2], Keith L. Obstein[1,3] and Nabil Simaan[1†]

***Abstract*— Colonoscopy demands multi-finger coordinated motion to achieve safe navigation. As a result, training for colonoscopists is challenging and skill assessment currently relies on subjective scoring by expert proctors. There is a need to provide tools for skill assessment and aid with training new interventionalists. This paper presents a new concept of an in-hand robotic mediation device that can be used for both skill assessment and training. The robotic device can be used to infer the kinematic motion as well as the power input of a user - both of which are proposed to be used for skill assessment and subtask skill classification. Preliminary results collected expert and novice users performing colonoscopy navigation are used to demonstrate this device as a skill assessment tool. A machine-learning model (classification and regression trees) is used for subtask classification of skill and evaluating the most important classification features. A user study demonstrates the effectiveness of this in hand haptic training and assessment tool. We believe that, in the future, this device will enable accelerated skill assessment and training and possible semi-automation of difficult maneuvers.**

***Index Terms*— Medical robotics, Colonoscopy, Skill Assessment, Haptic Device**

I. Introduction

Colonoscopy is an intervention involving the insertion and navigation of a long, flexible endoscope through the large intestinal tract, entering through the rectum and ending at the cecum. This procedure provides vital information for diagnosing and preventing colonic disease. In 2021, the American Cancer Society and United States Preventive Services Taskforce (USPSTF) lowered the recommended age for colon cancer screenings increasing demand for colonoscopies [1] and for trained endoscopists [2].

Learning to use a colonoscope is like learning to play a new musical instrument. It involves multi-fingered, synchronized manipulation of the two knobs and five buttons shown in Fig. 1. The scope is controlled completely by the left hand of the user, regardless of hand dominance. The right hand is reserved for feeding/rotating the colonoscope shaft into the body. Proper coordination of the forces applied on the knobs to maneuver the tip through the intestine can only be learned through prolonged, hands-on practice. This practice develops muscle memory to help the trainee learn the different finger motions necessary for safely controlling the colonoscope through a patient despite any variation in friction losses, motion transmission losses, and colon shape.

Colonoscopy training is based on the apprenticeship model that involves visual and verbal direction from expert users towards the trainee while the trainee performs colonoscopy on a patient. The apprenticeship model exposes patients to pure novices at a very early stage in their training. During difficult maneuvers, a trainee currently must surrender the device to an expert to demonstrate navigation. This process of tool handoff hinders educational progression and delays the development of muscle synergies needed to achieve these complex manipulations. Since skill acquisition for the colonoscope depends on developing muscle memory, verbal direction proves insufficient when conveying the nuanced sensory experience intrinsic to colonoscope navigation.

This training paradigm also burdens expert trainers by diverting time away from potential patient care. New endoscopists must complete approximately 200 supervised procedures to be considered minimally competent [3]. To address the need for resources, accelerating training, and skill assessment, this paper addresses the need for a skill assessment tool that in the future can also double as an expert trainer for colonoscopy or for semi-automating navigation.

The most related works to this paper lie in the domains of training tools and skill assessment measures for colonoscopy. Obstein et al. in [4] used motion tracking data of magnetic markers on a colonoscope shaft to assess user skill and to classify experts v.s. novices. The user's insertion force on the colonoscope shaft was also used in [5–7] as a means to assess skill. These works also were limited to consideration of skill assessment to the entire procedure.

Relative to prior works, we present what we believe is the first robotic mediation system for in-hand manipulation and skill assessment that is capable of capturing kinematic motion data of the colonoscope control wheels as well as the user's input torque. This provides the user's input power as an additional source of data for skill assessment, which is an extension of the use of energy for skill assessment as proposed by [8] within the context of laparoscopic surgery. We propose various kinematic and power measures and test their relevance to skill classification at a sub-task level consistent with navigating known segments of the colon. Finally, this design allows trainees to avoid device handoff and, in the future, it may be used for training, skill assessment and automated skill scoring.

† Corresponding author
[1]Department of Mechanical Engineering, Vanderbilt University, Nashville, TN 37235, USA (olivia.richards, nabil.simaan) @vanderbilt.edu
[2]Department of Computer Science, Vanderbilt University, Nashville, TN 37212, USA (jumanh.atoum, jieying.wu) @vanderbilt.edu
[3]Division of Gastroenterology, Hepatology and Nutrition, Vanderbilt University Medical Center, Nashville, TN 37232, USA (keith.obstein) @vumc.org

We limit the scope of this paper to presenting the design of the device (section II), the control and sensing model (section III), the experimental design (section IV), and skill assessment (section VI).

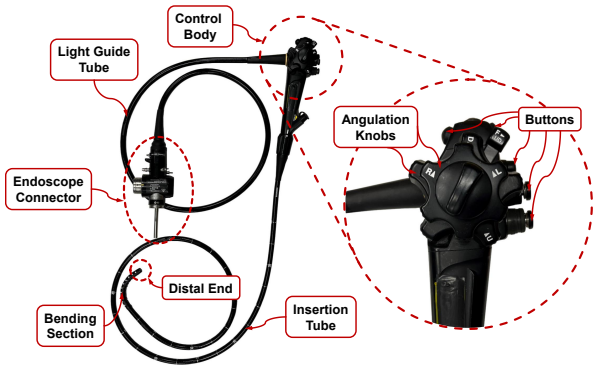

Fig. 1: A standard colonoscope showing the control wheels and buttons for aspiration, air/water feeding, and auxiliary image adjustment/freeze.

II. Design of Robotic Mediation Device

The robotic mediation device shown in Fig. 2 consists of two main mechanisms: the actuation unit and the adapted colonoscope control body. The system works in parallel with the user during operation. As the knobs are rotated, the robot actuates the corresponding motor to complete a desired task.

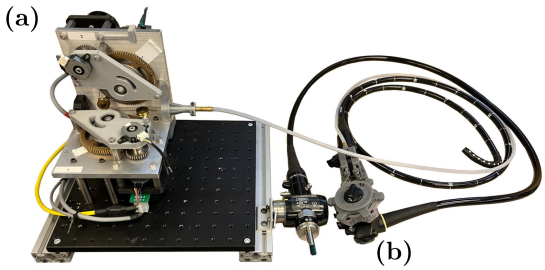

Fig. 2: Robotic mediation device: a) the actuation unit; b) the adapted control body of the colonoscope.

A. Actuation Unit

The actuation unit for the collaborative haptic system is comprised of two geared Maxon EC60 flat (625855) brushless motors with capstans for wire wrapping and tensioning as shown in Figure 3 (a). There are two identical actuator assemblies, one for each knob on the colonoscope. There is a 32/90 gear ratio from a 32-tooth stainless steel gear attached to the motor shaft and a 90-tooth brass gear to which the wire capstans are attached, as shown in Figure 3 (b).

Each motor connects to a wire-rope capstan via a custom series-elastic element made of ⌀2mm x 32.5mm superelastic NiTi torsion bar as shown in Fig 3 (c). The wire rope consists of seven bare 1x19 stainless steel strands (Carl Stahl Sava Industires PN: 103206). Each wire is ⌀0.8128mm and roughly 450cm. The rotation of the wire-rope capstan

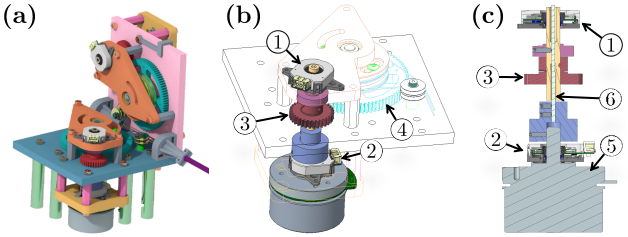

Fig. 3: CAD renderings of the haptic actuator. The full actuator assembly (a), the haptic components of one actuator assembly (b), and cross-section of an actuator showing the series-elastic element (c). The elastic element facilitates user torque estimation by measuring the angular deflection of a NiTi ⑥ bar. The differential angular positions of an ① absolute encoder and the motor's ② incremental encoder give the angular deflection from user torque. The motor ⑤ transmits motion to the control wheels through the 32-tooth stainless steel gear ③ to the larger brass gear ④.

is read via an absolute encoder (CUI Devices AMT222D-V 14 bit) while the rotation of the motor is read by an incremental encoder (CUI Devices AMT10E2-V 5120 PPR). The differential read between these encoders determines the torsional deflection of the torsion bar. The torsion bar serves the triple purpose of providing a means to estimate user input torque in addition to facilitating actuation transmission while allowing user intent detection of wheel rotation. More details about these functions are provided in the section III.

The torsional bar design parameters were determined by first measuring the typical maximal actuation torque at the control wheels of the colonoscope. This torque was experimentally measured to be 530Nmm. The torsion bar has to transmit this torque divided by the gear ratio of 90/32, which results in a maximal torque transmission of 188.4Nmm.

We specified the desired torsional deflection corresponding with this maximal torque to be 6 degrees. This choice was made to strike a balance between the need to have a sufficiently stiff transmission so the user does not feel a degradation in motion transmission and a sufficiently flexible shaft to have good sensitivity for torque estimation from shaft deflection. Upon design iterations checking shaft natural frequency, Von-Mises static failure safety factor, and maximal strain of less than 1%, we selected a shaft 2.0mm in diameter with a torsional trasnmission length of 32.5mm. With the assumption of an encoder with 5120 CPT and quadrature results in a torque sensing sensitivity of $0.196\frac{\text{Nmm}}{\text{count}}$.

The torsional stiffness k_s of a round bar is given by $\mathrm{k}_s = G\pi d^4/32L$ With the above diameter $d = 2.0$mm and length parameter $L = 32.5$mm, and assuming a Young's modulus of 65Gpa and a shear modulus $G = 24.43$Gpa, the nominal torsional stiffness is $20.6\frac{\text{mNm}}{\text{degree}}$ or $1.18105\frac{\text{Nm}}{\text{rad}}$.

The sensed torque τ as a function of the absolute[1] q_{abs}

[1]For notation simplicity, we assume that q_{abs} is the change in absolute encoder reading relative to when the code was started with incremental encoder values being reset to zero.

and incremental q_{inc} encoder readings is given by:

$$\tau = k_s \underbrace{(q_{abs} - q_{inc})}_{\eta} = k_s \eta. \quad (1)$$

B. Adapted Control Body

The adapted control body had two SLA printed wheels press-fit onto the original control wheels of the colonoscope. The printed wheels included capstans that connected the control wheels to the motors using wrapped wire ropes. Actuation transmission is passed from the actuation unit to the control body via a multi-lumen Teflon tubing for minimized friction. The wire ropes are directed from the Teflon tube to the control wheel capstans using a mounted pulley mechanism as shown in Fig.4.

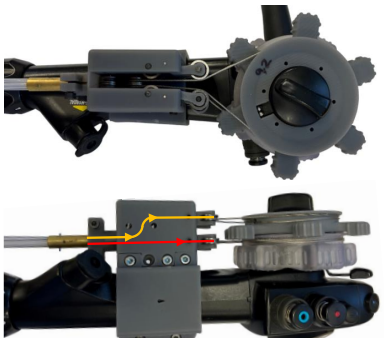

Fig. 4: The adapted control body of the colonoscope. The wire paths are shown on the left using colored lines.

III. Sensory and Control Approach

A successful control framework for the colonoscope requires estimating the user's rotational intent and input power/torque, capturing the required motor torques necessary to bend the colonoscope in each configuration, and applying a variable admittance control. The control law must grant the user control of the colonoscope while reserving the option to implement virtual fixtures limit bending or offer haptic cues to help the user with a specific task. To achieve this, we devised a tiered control strategy for robotic mediation. A high-level admittance controller (HLC) determines the user's intended direction of motion and uses the deflection of the torsion bar to output a joint-level reference signal. This output is fed through a mid-level PID position controller (MLC) that outputs a torque control reference τ_{ref} to an embedded joint-level low-level controller (Maxon EPOS2 50/5) via CANopen communication protocol. The HLC and MLC control framework, data-logging, and communication with sensors during the user study were implemented using Simulink Real-Time 2017b with a control rate of $500Hz$.

A. User power, torque, and intent

The torque on each colonoscope control wheel is a sum of the actuation torque on the capstans $\boldsymbol{\tau}_{capstan} \in \mathbb{R}^2$ and the user torques $\boldsymbol{\tau}_{user} \in \mathbb{R}^2$ and is equal to the torque $\boldsymbol{\tau}_{colonoscope} \in \mathbb{R}^2$ needed to bend the colonoscope at a given configuration specified by motor joint values $\mathbf{q} = [q_1, q_2]^{\mathrm{T}}$:

$$\boldsymbol{\tau}_{colonoscope} = \boldsymbol{\tau}_{user} + \boldsymbol{\tau}_{capstan} \quad (2)$$

In the following, we assume that a feed-forward torque term $\boldsymbol{\tau}_{ff} \in \mathbb{R}^2$ is available to approximate the colonoscope torque, i.e., $\boldsymbol{\tau}_{ff} \approx \boldsymbol{\tau}_{colonoscope}$. Using the motor torques $\boldsymbol{\tau} \in \mathbb{R}^2$, the motor-to-capstan gear ratio g_1 and the wire-rope capstan transmission ratio g_2 , we can write $\boldsymbol{\tau}_{capstan} = \boldsymbol{\tau} g_1 g_2$ and pproximate user torque as:

$$\boldsymbol{\tau}_{user} \approx \boldsymbol{\tau}_{ff} - \boldsymbol{\tau} g_1 g_2 \quad (3)$$

Using the known stiffness of the torsional bar k_s, we can relate the feed-forward torque as a function of an expected torsional deflection $\tilde{\boldsymbol{\eta}}$:

$$\boldsymbol{\tau}_{ff} = \tilde{\boldsymbol{\eta}} k_s g_1 g_2 \quad (4)$$

which results in the estimate for the user torque input:

$$\boldsymbol{\tau}_{user} \approx (\tilde{\boldsymbol{\eta}} - \boldsymbol{\eta})\, k_s g_1 g_2. \quad (5)$$

where $\boldsymbol{\eta}$ is the measured deflection of the torsion bar.

Using the above result and the control wheel angular speed we can estimate the user's input power to the system as:

$$p = \boldsymbol{\omega}^{\mathrm{T}} \boldsymbol{\tau}_{user} \approx \dot{\mathbf{q}}^{\mathrm{T}} (\tilde{\boldsymbol{\eta}} - \boldsymbol{\eta})\, k_s g_1^2 g_2^2 \quad (6)$$

where $\boldsymbol{\omega} \in \mathbb{R}^2$ denotes the vector of angular speeds of the colonoscope control wheels.

The user's intent in rotating the control wheels is determined using the temporal rates of change $\dot{\eta}_i$, $i = 1, 2$, of the torsional bar deflections. We assume that the user's inputs torque is sufficiently large to overcome friction in the wire-rope transmission and induce a change in the torsional deflection. The incremental change in torsional bar deflection is calculated using a moving average filter over n_{cycles}

$$\triangle \eta_i = \sum_{j=1}^{n} \frac{\dot{\eta}_i dt}{n_{cycles}} \quad (7)$$

We use the sign of $\triangle \eta_i$ to determine the sense of direction that the user intends to rotate the control wheel. In the admittance control section below both $sign(\triangle \eta)$ and the absolute value of $\dot{\eta}$ are used to follow a user's intent in rotating each wheel.

Finally, assuming a responsive tuning for the admittance controller, the difference $(\tilde{\boldsymbol{\eta}} - \boldsymbol{\eta})$ can be assumed almost constant and the user's input power becomes proportional to the angular speed $\boldsymbol{\omega}$ of the control wheels.

B. Estimating motor torques to bend the colonoscope

For each motor, the torque τ_{ff_i}, $i = 1, 2$ was obtained experimentally in which we bent the colonoscope by rotating the motors to a known $\mathbf{q}$ joint value and read the motor current from the low-level motor controller (which was set in current mode). Using Eq.(4), these values were converted to torsional deflections $\eta_i(\mathbf{q})$, $i = 1, 2$. The value of $\eta_i(\mathbf{q})$ were saved for a collection of monotonously-ordered and distinct joint value sets $\mathcal{Q}_1 \triangleq \{q_{1_1}, q_{1_2}, \ldots, q_{1_n}\}$ and $\mathcal{Q}_2 \triangleq$

$\{q_{2_1}, q_{2_2}, \ldots, q_{2_m}\}$ following Algorithm 1 and produced two experimental data matrices $\mathbf{\Phi}_i$, $i = 1, 2$:

$$\mathbf{\Phi}_i = \begin{bmatrix} \eta_i(q_{1_1}, q_{2_1}) & \cdots & \eta_i(q_{1_1}, q_{2_m}) \\ \vdots & \ddots & \vdots \\ \eta_i(q_{1_n}, q_{2_1}) & \cdots & \eta_i(q_{1_n}, q_{2_m}) \end{bmatrix} \tag{8}$$

Algorithm 1 Defining Φ_1 and Φ_2

```
q_vec = −100:20:100
for q_1 = q_vec do
    for q_2 = q_vec do
        Φ1(j, k) = η1(q_1j, q_2k)
        Φ2(j, k) = η2(q_1j, q_2k)
    end for
end for
```

Since each element of $\boldsymbol{\tau}_{ff}$ is a function of the colonoscope configuration as determined by the joint values $\mathbf{q}$, we decided to use a double modal interpolation approach to fit a modal function series to the experimental data. Using the approach in [9] we derived the modal interpolation maps as:

$$\tilde{\eta}_i(q_1, q_2) = \boldsymbol{\psi}(q_1)^T \mathbf{A}_i \boldsymbol{\theta}(q_2), \quad i = 1, 2 \tag{9}$$

where $\boldsymbol{\psi}(q_1)$ and $\boldsymbol{\theta}(q_2)$ specified as monomial bases:

$$\boldsymbol{\psi}(q_1) = [1, q_1, q_1^2, \ldots, q_1^{v-1}]^T \in \mathbb{R}^v \tag{10}$$

$$\boldsymbol{\theta}(q_2) = [1, q_2, q_2^2, \ldots, q_2^{w-1}]^T \in \mathbb{R}^w \tag{11}$$

The above monomial bases remain well conditioned below degree 6, [10] and one could choose another set of orthogonal functions such as Chebyshev polynomials [11].

Using (9) for all the experimental data collected in $\mathbf{\Phi}_i$ results in the following linear matrix equation with the modal coefficients matrix $\mathbf{A}_i$ as the unknown:

$$\mathbf{\Phi}_{i_{n\times m}} = \mathbf{\Omega}_{n\times v} \mathbf{A}_{i_{v\times w}} \mathbf{\Gamma}_{w\times m} \tag{12}$$

where $\mathbf{\Omega}_{n\times v}$ and $\mathbf{\Gamma}_{w\times m}$ are the following matrices given by substituting experimental value pairs in $\mathcal{Q}_1$ and $\mathcal{Q}_2$:

$$\mathbf{\Omega}_{n\times v} = \begin{bmatrix} 1 & q_{1_1} & q_{1_1}^2 & \cdots & q_{1_1}^{v-1} \\ 1 & q_{1_2} & q_{1_2}^2 & \cdots & q_{1_2}^{v-1} \\ \vdots & \vdots & \ddots & \vdots & \\ 1 & q_{1_n} & q_{1_n}^2 & \cdots & q_{1_n}^{v-1} \end{bmatrix} \tag{13}$$

$$\mathbf{\Gamma}_{w\times m} = \begin{bmatrix} 1 & 1 & \cdots & 1 \\ q_{2_1} & q_{2_2} & \cdots & q_{2_m} \\ \vdots & \vdots & \ddots & \vdots \\ q_{2_1}^{w-1} & q_{2_2}^{w-1} & \cdots & q_{2_m}^{w-1} \end{bmatrix} \tag{14}$$

Equation (12) can be re-cast as a linear equation with a vector as an unknown using Kroneker product [12]:

$$\left[\mathbf{\Gamma}^{\mathrm{T}} \otimes \mathbf{\Omega}\right] Vec(\mathbf{A}_i) = Vec(\mathbf{\Phi}_i) \tag{15}$$

where $\otimes$ denotes the Kronecker matrix product and the Vec operator is given by $Vec(\mathbf{A})_{m\times n} \triangleq [a_{11} \cdots a_{m1}, a_{12} \cdots a_{m2}, \cdots, a_{1n} \cdots a_{mn}]^{\mathrm{T}}$. The above equation is solved for $\mathbf{A}_i$ using:

$$Vec(\mathbf{A}_i) = \left[\mathbf{\Gamma}^{\mathrm{T}} \otimes \mathbf{\Omega}\right]^{\dagger} Vec(\mathbf{\Phi}_i) \tag{16}$$

where $()^{\dagger}$ denotes the Moore-Penrose pseudo-inverse.

Once $\mathbf{A}_i$ is reconstituted from $Vec(\mathbf{A}_i)$, it can be used in (9) to provide an interpolation map for $\tilde{\eta}_i$. By using (4), we also obtain the corresponding element τ_{ff_i}.

C. Active Compliance Control

The HLC implemented a high-level admittance control law that used the following equation to update the control reference to the MLC:

$$\boldsymbol{q}_{i+1} = \boldsymbol{q}_i + \dot{\boldsymbol{q}}_{i+1} dt \tag{17}$$

where q_{i+1} and $\dot{q}_{i+1}$ are the desired position and velocity of the incremental encoder, q_i is the current incremental encoder position, and dt is the controller's sample time (0.002 seconds). The reference signal for joint-level desired speed is updated based on the user's input and the error in expected torques at given positions. We therefore include two terms $\dot{q}_{ff}$ and $\dot{q}_{adm}$ to address these two needs:

$$\dot{\boldsymbol{q}}_{i+1} = \dot{\boldsymbol{q}}_{adm} + \dot{\boldsymbol{q}}_{ff} \tag{18}$$

Given the user's intended rotation direction as indicated by $sign(\triangle\eta)$, we use a variable proportional gain feedback law:

$$\dot{\boldsymbol{q}}_{adm} = K_a K_s \,\mathrm{sgn}(\triangle\boldsymbol{\eta}) |\dot{\boldsymbol{\eta}}| \tag{19}$$

where K_a is the admittance gain, K_s is the torsional bar stiffness constant, and $|\dot{\eta}|$ is used to scale the admittance to allow the motor to follow the user's input torque proportionally to the induced torsion.

The feed-forward term $\dot{q}_{ff}$ is also determined by a proportional gain feedback taking into account the user's intended motion direction and the error between the current torsional bar deflection and the feed-forward (expected) torque needed to bend the colonoscope.

$$\dot{\boldsymbol{q}}_{ff} = \mathrm{sgn}(\triangle\boldsymbol{\eta}) K_{ff} K_a |\boldsymbol{\tau}_{ff} - \boldsymbol{\tau}_{cur}| \tag{20}$$

where the current motor torque was calculated as:

$$\boldsymbol{\tau}_{cur} = \boldsymbol{\eta} K_s \tag{21}$$

and the feed-forward motor torque was calculated as:

$$\boldsymbol{\tau}_{ff} = \tilde{\boldsymbol{\eta}} K_s \tag{22}$$

IV. Experimental Design

To understand the relationship between skill level and torque/work input, a user study with five participants was conducted to record data characterizing their interactions with the colonoscope while maneuvering it through a simplified replica of a human colon.

Fig. 5: (Right) Picture taken while collecting data from the expert user. (Left) The silicon model of a colon with numbered landmarks indicating the different segments of the intestine: ① starting location; ② rectum→sigmoid colon; ③ sigmoid→descending colon; ④ descending→transverse colon; ⑤ transverse→ascending colon ; ⑥ ascending colon→cecum.

A. Setup and Materials

The experiments, shown in Fig. 5, used an Olympus CV-180 & CLV-180 Evis Exera II endoscopy system for imaging and illumination. The Kyoto Kagaku [13] colon model was enclosed in a foam block and placed beneath the monitor displaying the live video from the tip of the scope.

The position and orientation of the colonoscope insertion tube were recorded using a 3D Guidance trakSTAR 2 system with four 6DOF magnetic sensors. Three sensors were Model 130 and the furthest sensor from the tip was a Model 90. The difference in model number was only due to availability and did not change the collected data. These sensors were positioned 10 centimeters apart starting from the tip of the scope. The sensors communicated their position relative to the Ascension Flat Metal Immune Transmitter, which was placed beneath the colon model during experiments.

To quantify user torque and work, the absolute and incremental encoder data were recorded using Simulink Real-Time with a control cycle frequency set at 500Hz. The encoders' position and velocity at each cycle were logged.

B. Experimental Protocol and Procedure

The center-line of the intestine was digitized by tracing a magnetic marker. Similarly, the entrance to the colon was manually digitized along with select positions marked by an expert gastroenterologist. These markers are shown in Fig. 5 along with the corresponding segments of the colon.

We then asked four novice users and one clinical expert (all co-authors on this exploratory study) to carry out ten insertions of the colonoscope navigating from the rectum to the cecum. In an attempt to replicate the conditions of an actual colonoscopy, the phantom and insertion tube were generously lubricated using a standard water-based lubricant. During the novice runs, the phantom was covered to encourage them to rely on the monitor instead of the phantom for navigation. Prior to recording data, each participant was allowed multiple practice runs to familiarize themselves with the basics of colonoscope control and to adjust to using the robotic mediation device. Multimedia Extension I shows our device and our robotic mediation device in use.

Specific instructions were given to users before data collection. These instructions described experimental requirements and prohibited actions. To be considered a successful run, the user had to start by visualizing an internal seam in the silicon positioned between the model's opening and the rectum. After the seam was in view, the data collection began. To advance the scope, the user first needed to center intestinal tunnel on the monitor. This constraint was set to inhibit the user from ramming the colonoscope against the colon walls as a way to passively navigate the scope. This technique is incorrect and unsafe because it relies solely on the colon's corners and curves for steering and can result in colonoscope looping, intestinal bunching, or, in severe cases, intestinal perforation. The run was concluded once the cecum was reached and the cecum was successfully visualized.

The data was saved after the cecum was visualized. The data collected included: 1) position and velocity for incremental and absolute encoders; 2) position and orientation for the four magnetic sensors; and 3) elapsed time.

V. Data Processing and Experimental Results

The data collected was post-processed to include calculations of the torsional shaft deflections η_i, the user torques τ_i on the control wheels, and user input power. Because the control and data logging code ran at 500Hz and the magnetic tracker information came at 100Hz via UDP, the data was processed to remove repeated readings and truncated based on the closest point to the entry point of the colon (designating the start of insertion). Data was also resampled to include 1000 readings for each user to ensure equidistant arc-length spacing and avoid biasing any classification results with different spatial data densities per a unit-length of the colon. The resampling was achieved using Piecewise Cubic Hermite Interpolating Polynomials and visualized against the original data to ensure that the interpolation re-sampling does not produce any meaningful variations in the data.

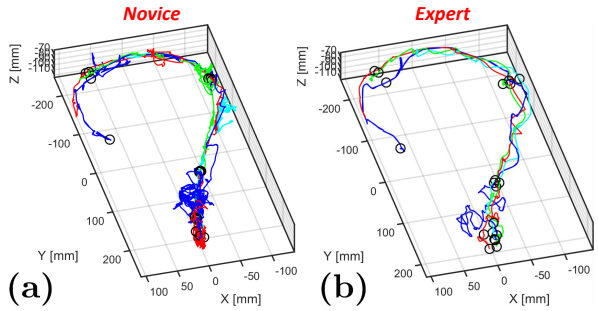

Fig. 6: (a) The path of each sensor for a novice user during a procedure. (b) The path of each sensor for an expert user. The blue, red, green, and cyan lines represent sensors 1-4, respectively. The black circles identify each path's transition between the intestine's segments.

For each user insertion experiment, the motion traces of each marker were plotted in Fig. 6 and the local tangents are plotted in Fig. 7. We computed the local tangents of the nominal centerline from the digitized centerline data to

establish a comparitive basis of each user's motion traces. At each point of a user's motion trace, the closest point to the nominal centerline was computed as well as the dot product between the corresponding local tangents. Additionally, the arc length in each colon segment was computed and compared between the user's motion traces and the centerline.

Using the local tangent data for the marker motion traces, we computed the orientation change $\Delta\mathbf{R}$ of the local marker frame relative to the orientation of the same marker at the colon entrance (denoted as $\mathbf{R}_{entrance}$). This orientation change was computed as a spatial rotation sequence where $\mathbf{R}_{current} = \Delta\mathbf{R}\,\mathbf{R}_{entrance}$. Solving for $\Delta\mathbf{R}$ and finding the axis angle parametrization [2] $\Delta\mathbf{R} = e^{[\hat{\mathbf{n}}]^\wedge\gamma}$ yields the unit vector of axis of rotation $\hat{\mathbf{n}}$ and the rotation angle γ. Figure 8 shows the rotation axes unit vectors color-coded by each segment of the colon for both the expert and the novice. For each set of unit vectors per colon segment also computed the average direction and displayed it as a scaled-up vectors as shown in the same figure. The deviation of each local tangent relative to the segment average direction unit vector was also calculated.

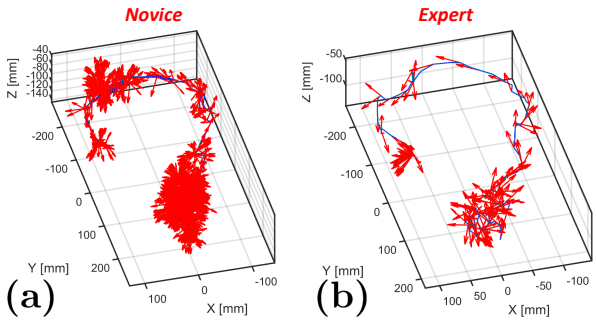

Fig. 7: The path of the first sensor and the local tangent along the path for (a) a novice user, and (b) an expert user. Local tangents were plotted every 2 points along the path.

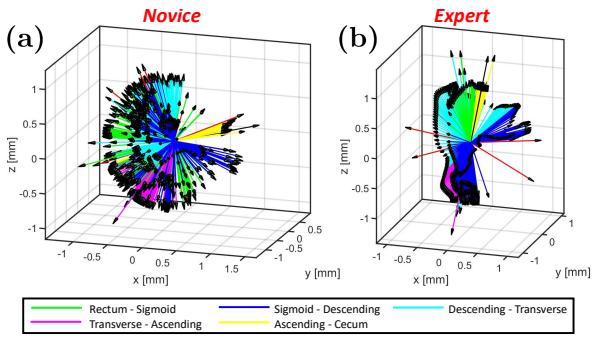

Fig. 8: The variation of the axis of rotation throughout the procedure for sensor 1. The arrow's color corresponds to a segment of the intestine at the time of reading.

VI. Skill Assessment

To gain understanding of user performance, we performed our user skill assessment using subjective measures and objective classification. The subjective observations serve to visualize the observed difference between the novice performance and the expert while the objective assessment serves to provide classification of user skill per each segment of the colon and also aims to identify which of the computed parameters best improves the classification scores.

[2]The notation $[\mathbf{x}]^\wedge$ denotes the cross-product matrix of vector $\mathbf{x}$.

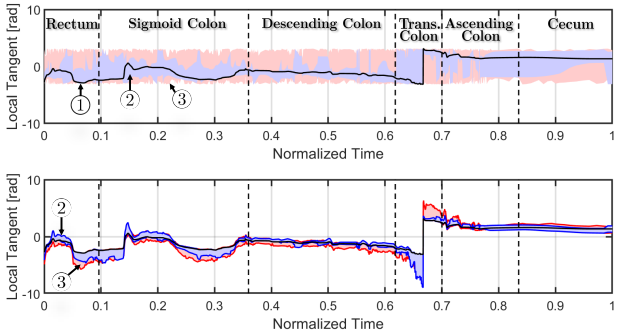

Fig. 9: The tangent angle of the colonoscope's tip projected onto the x-y plane for all experiments. Expert data was plotted with a blue shaded region ② and the novice's plotted with a red ③ using [14]. (Top) Maximum deviation for both groups with the anatomical centerline shown with a black line ①. (Bottom) Average deviation of the users from the centerline's angle using the same designated colors.

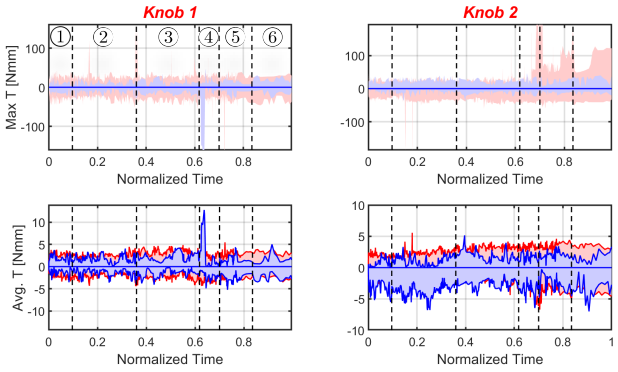

Fig. 10: The torque on each knob for all experiments. Expert data is plotted with a blue shaded region and the novice's is plotted with a red using [14]. (Top) Maximum torque applied by each group. (Bottom) Average torque applied. Each intestinal segment is represented using numbers matching the order shown in 9

A. Subjective Assessment

An example of the difference in path length between expert and novice users is shown in Fig. 6. The expert user performed the procedure in a path with fewer corrective maneuvers than the novice users. The Rectum to Sigmoid Colon segment proved to be the most challenging which is represented in 6 with the dense network of sensor signals crowded near the starting position. The expert user was able to navigate through this portion with significantly fewer corrections than the user.

The instantaneous direction of motion along the path is represented in Fig. 7 for expert and novice users. The expert user's direction followed the centerline of the model closer, showing minimal directional deviation. The close proximity of tangent lines identifies challenging features along the path. Many arrows at a single location that diverge from the model's natural curvature show consecutive redirection and course correction. Fig. 7 shows that these features were more prominent in the novice data than the experts.

The orientation of the axis of rotation was analyzed and the results in Fig. 8 show the expert user's ability to orient the colonoscope through each segment of the intestine smoothly. The novice user's orientations appeared almost random and showed significant variation within each segment as well as no clear transitions between them.

Torque readings shown in 10 display a wider range of maximum torques applied for novice users. This was inferred as being sudden movements during course corrections. The average torque for the expert showed a smaller band of variation displaying more efficient control.

B. Objective Assessment

We assess users' skill levels using their experimental performance. We use decision trees to classify skill levels based on input parameters and identify which features contribute to the behavior of experts and novices. We choose classification and regression trees (CART) due to their ease of interpretation for humans and their comparable accuracy to other classification models [15], [16]. CART involves creating a binary decision tree by analyzing a training dataset where correct classifications are known. At each step, the algorithm splits the data into two sub-groups based on one specific input data feature, forming branches in the tree. As the process continues, the number of entities in each sub-group decreases, thus requiring a sufficiently large training sample for accurate results [17]. This aids human interpretability as the number of trees that split on a specific feature denotes how important the feature is to classification (ie. the more trees that split on it, the more important the feature). Additionally, tree branch thresholds show the ranges that lead to a more likely novice or expert classification.

For evaluation, we used two cross-validation techniques, leave-one-user-out and leave-one-trial-out. Leave-one-user-out evaluation includes training the decision tree on all users and leaving one novice out, whereas leave-one-trial-out excludes one random trial from each user for evaluation. Our sample size is large enough to train the decision tree since each user has 10 trials. The 8^{th} trial for the expert user and the 9^{th} trial for novice 2 were removed because of errors during data collection.

We examined the most prominent features given by the decision tree for each user at each segment as seen in table I. For all participants, the Δ Segment length is the feature that contributes the most to novice behavior. Also, Δ Segment length feature is the only feature required for classifying participants for Segment 3 based on their skill level.

In Fig. 11 we showed how close each novice is to expert's behavior based on the classifier's inability to distinguish between the novice's behavior and the expert's behavior. The classifier can distinguish skill levels with an average accuracy of 91% across all novices, it is achieving the highest accuracy on Segments 3 and 4 for all novices while scoring the lowest accuracy on Segments 1 and 5.

We also computed the dice coefficient by computing the number of positive as well as penalizing for false positive predictions, this is given by the encircled numbers in Fig. 12. The dice coefficient values go in hand with the results from evaluating through leaving one user out, where Segments 1 and 5 have the lowest dice scores while Segments 3 and 4 have the highest dice scores.

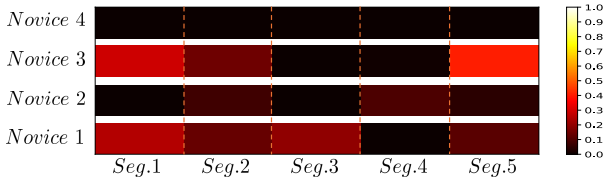

Fig. 11: Color-bar charts of novice skill progression as a function of each colon segment. 1 designates expert skill level. 0 designates novice skill level.

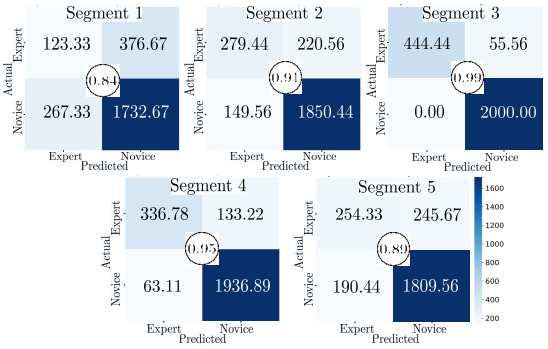

Fig. 12: Confusion matrices for each segment across all users. The encircled number provides the dice scores.

VII. Conclusion

This paper presented a novel haptic mediation device capable of serving as a tool for skill assessment, accelerated skill acquisition via haptic training, and as a semi-automation robotic navigation assistant. This device is the first tool that offers these functions for in-hand finger manipulations that involve complex digit manipulation synergies. It also provides estimates of the user's input torque and power and intended motions. These added signals allowed classification of user skill for anatomical segments of the colon. We presented a modeling and control approach that allows the user to remain in control of the device while deducing the user's motion intent and to applying variable admittance with assistive effort offsetting the moment needed to bend the colonoscope. We also demonstrated the first exploratory use of this device for skill assessment. The types of signals

TABLE I: The five most prominent features are shown with their values for all novice participants at each segment. Δ Segment length is the arc-length difference per segment relative to the colon centerline, $x_{marker\ i}$ is the x coordinate for the i^{th} marker, $Average_{marker_i}$ is the average dot product between the path tangent and the average direction of the path tangent for the i^{th} segment, p_i is the power input on the i^{th} control wheel.

Participants	Segment 1		Segment 2		Segment 3		Segment 4		Segment 5	
Novice 1	Δ Segment length	0.65	Δ Segment length	0.66	Δ Segment length	1.00	Δ Segment length	0.92	Δ Segment length	0.62
	$z_{\text{marker 2}}$	0.14	$x_{\text{marker 2}}$	0.12	$x_{\text{marker 2}}$	0.00	$Average_{\text{marker 1}}$	0.08	τ_1	0.24
	$y_{\text{marker 1}}$	0.07	Average	0.10	$Average_{\text{marker 2}}$	0.00	$x_{\text{marker 2}}$	0.00	p_1	0.06
	$z_{\text{marker 1}}$	0.05	$Average_{\text{marker 1}}$	0.03	$Average_{\text{marker 1}}$	0.00	$Average_{\text{marker 2}}$	0.00	$\gamma_{\text{marker 1}}$	0.03
	$x_{\text{marker 2}}$	0.04	$x_{\text{marker 1}}$	0.02	$x_{\text{marker 1}}$	0.00	$x_{\text{marker 1}}$	0.00	$Average_{\text{marker 1}}$	0.02
Novice 2	Δ Segment length	0.51	Δ Segment length	0.56	Δ Segment length	1.00	Δ Segment length	1.00	Δ Segment length	0.69
	$y_{\text{marker 1}}$	0.15	$x_{\text{marker 2}}$	0.13	$x_{\text{marker 2}}$	0.00	$x_{\text{marker 2}}$	0.00	τ_1	0.23
	$z_{\text{marker 2}}$	0.11	$Average_{\text{marker 2}}$	0.08	$Average_{\text{marker 2}}$	0.00	τ_1	0.00	p_1	0.05
	$x_{\text{marker 1}}$	0.08	$Average_{\text{marker 1}}$	0.05	$Average_{\text{marker 1}}$	0.00	p_1	0.00	$\gamma_{\text{marker 1}}$	0.02
	$Average_{\text{marker 2}}$	0.05	$y_{\text{marker 1}}$	0.04	$y_{\text{marker 1}}$	0.00	$\gamma_{\text{marker 1}}$	0.00	$x_{\text{marker 1}}$	0.01
Novice 3	Δ Segment length	0.57	Δ Segment length	0.78	Δ Segment length	1.00	Δ Segment length	0.87	Δ Segment length	0.72
	$z_{\text{marker 2}}$	0.15	$Average_{\text{marker 2}}$	0.10	$Average_{\text{marker 2}}$	0.00	$x_{\text{marker 1}}$	0.07	$Average_{\text{marker 1}}$	0.24
	$z_{\text{marker 1}}$	0.08	$Average_{\text{marker 1}}$	0.03	$Average_{\text{marker 1}}$	0.00	$x_{\text{marker 2}}$	0.07	$y_{\text{marker 1}}$	0.01
	p_2	0.07	$y_{\text{marker 1}}$	0.03	$y_{\text{marker 1}}$	0.00	$Average_{\text{marker 2}}$	0.00	$x_{\text{marker 1}}$	0.01
	$\gamma_{\text{marker 2}}$	0.06	p_2	0.02	p_2	0.00	$Average_{\text{marker 1}}$	0.00	p_1	0.01
Novice 4	Δ Segment length	0.53	Δ Segment length	0.75	Δ Segment length	1.00	Δ Segment length	0.92	Δ Segment length	0.59
	$y_{\text{marker 1}}$	0.14	$Average_{\text{marker 2}}$	0.08	$Average_{\text{marker 2}}$	0.00	$Average_{\text{marker 1}}$	0.08	τ_1	0.27
	$z_{\text{marker 2}}$	0.11	$Average_{\text{marker 1}}$	0.04	$Average_{\text{marker 1}}$	0.00	$Average_{\text{marker 2}}$	0.00	p_1	0.05
	$Average_{\text{marker 2}}$	0.09	$y_{\text{marker 1}}$	0.03	$y_{\text{marker 1}}$	0.00	$y_{\text{marker 1}}$	0.00	$Average_{\text{marker 1}}$	0.03
	$x_{\text{marker 1}}$	0.04	τ_2	0.02	τ_2	0.00	τ_2	0.00	$\gamma_{\text{marker 1}}$	0.03

collected via our device are novel within the context of skill assessment for colonoscopy and offer a glimpse at differences between novices and the single expert in this exploratory study. It was shown that novices exhibit longer tool traversal paths, erratic tool-tip angulation, poor orientation when following the centerline of the colon, longer times, and erratic changes in user torque/effort. We also carried out a classification study using classification and regression trees. The classification study also elucidated the five most prominent features aiding with high classification accuracy. This exploratory study has limitations, the most significant being the number of expert users. An IRB-approved study involving non-author subjects and with a higher number of experts and novices and with the most prominent variations of the colon anatomy needs to be carried out to strengthen validation of our tool and skill assessment methods. The modeling and control strategy neglects dynamics and lumps frictional effects as part of experimental calibration. Nevertheless, we believe that this exploratory effort addresses important applications that may accelerate training of endoscopists and also offer a future use of tandem training allowing an expert to "nudge" a trainee by using a similar device coupled by software to the trainee's tool.

REFERENCES

[1] K. W. Davidson, M. J. Barry, C. M. Mangione, M. Cabana, A. B. Caughey, E. M. Davis, K. E. Donahue, C. A. Doubeni, A. H. Krist, M. Kubik, *et al.*, "Screening for colorectal cancer: Us preventive services task force recommendation statement," *Jama*, vol. 325, no. 19, pp. 1965–1977, 2021.

[2] D. A. Joseph, R. G. Meester, A. G. Zauber, D. L. Manninen, L. Winges, F. B. Dong, B. Peaker, and M. van Ballegooijen, "Colorectal cancer screening: estimated future colonoscopy need and current volume and capacity," *Cancer*, vol. 122, no. 16, pp. 2479–2486, 2016.

[3] D. O. Faigel, T. H. Baron, B. Lewis, B. Peterson, J. Petrini, J. W. Popp, J. A. DiPalma, I. M. Pike, and I. L. Flax, "Ensuring competence in endoscopy." [Online]. Available: www.asge.org

[4] K. L. Obstein, V. D. Patil, J. Jayender, R. S. J. Estépar, I. S. Spofford, B. I. Lengyel, K. G. Vosburgh, and C. C. Thompson, "Evaluation of colonoscopy technical skill levels by use of an objective kinematic-based system," *Gastrointestinal endoscopy*, vol. 73, no. 2, pp. 315–321, 2011.

[5] L. Y. Korman, L. J. Brandt, D. C. Metz, N. G. Haddad, S. B. Benjamin, S. K. Lazerow, H. L. Miller, D. A. Greenwald, S. Desale, M. Patel, *et al.*, "Segmental increases in force application during colonoscope insertion: quantitative analysis using force monitoring technology," *Gastrointestinal endoscopy*, vol. 76, no. 4, pp. 867–872, 2012.

[6] A. R. Ende, P. De Groen, B. L. Balmadrid, J. H. Hwang, J. Inadomi, T. Wojtera, V. Egorov, N. Sarvazyan, and L. Korman, "Objective differences in colonoscopy technique between trainee and expert endoscopists using the colonoscopy force monitor," *Digestive diseases and sciences*, vol. 63, pp. 46–52, 2018.

[7] L. Y. Korman, V. Egorov, S. Tsuryupa, B. Corbin, M. Anderson, N. Sarvazyan, and A. Sarvazyan, "Characterization of forces applied by endoscopists during colonoscopy by using a wireless colonoscopy force monitor," *Gastrointestinal endoscopy*, vol. 71, no. 2, pp. 327–334, 2010.

[8] B. Poursartip, M.-E. LeBel, R. V. Patel, M. D. Naish, and A. L. Trejos, "Energy-based metrics for laparoscopic skills assessment," in *2016 38th Annual International Conference of the IEEE Engineering in Medicine and Biology Society (EMBC)*. IEEE, 2016, pp. 2648–2651.

[9] J. Zhang, J. T. Roland, S. Manolidis, and N. Simaan, "Optimal path planning for robotic insertion of steerable electrode arrays in cochlear implant surgery," *Journal of Medical Devices*, vol. 3, pp. 011 001–1–011 001–10, 2009.

[10] J. Angeles and C. S. López-Cajún, *Optimization of cam mechanisms*. Springer Science & Business Media, 2012, vol. 9.

[11] J. C. Mason and D. C. Handscomb, *Chebyshev polynomials*. Chapman and Hall/CRC, 2002.

[12] J. Brewer, "Kronecker products and matrix calculus in system theory," *IEEE Transactions on circuits and systems*, vol. 25, no. 9, pp. 772–781, 1978.

[13] A. M. Plooy, A. Hill, M. S. Horswill, A. S. G. Cresp, M. O. Watson, S.-Y. Ooi, S. Riek, G. M. Wallis, R. Burgess-Limerick, and D. G. Hewett, "Construct validation of a physical model colonoscopy simulator," *Gastrointestinal Endoscopy*, vol. 76, no. 1, pp. 144–150, 2012.

[14] K. Kearney, "boundedline.m," GitHub, Dec 2022, retrieved March 14, 2024.

[15] L. Breiman, *Classification and regression trees*. Routledge, 2017.

[16] T.-S. Lim, W.-Y. Loh, and Y.-S. Shih, "An empirical comparison of decision trees and other classification methods," Technical Report 979, Department of Statistics, University of Wisconsin, Madison, Tech. Rep., 1997.

[17] G. J. McLachlan, *Discriminant analysis and statistical pattern recognition*. John Wiley & Sons, 2005.